Published in final edited form as:
Circulation. 2009 April 21; 119(15): 2086–2095. doi:10.1161/CIRCULATIONAHA.108.826230.

Microarray Identifies Extensive Downregulation of Noncollagen Extracellular Matrix and Profibrotic Growth Factor Genes in Chronic Isolated Mitral Regurgitation in the Dog

Junying Zheng, PhD[1], **Yuanwen Chen, MD, PhD**[1], **Betty Pat, PhD**[1], **Louis A Dell'Italia**[1], **Michael Tillson, DVM**[3], **A Ray Dillon, DVM**[3], **Pamela Powell, BS, MS**[1], **Ke Shi, MD**[1], **Neil Shah, MS**[1], **Thomas Denney, PhD**[4], **Ahsan Husain, PhD**[1,2], and **Louis J Dell'Italia, MD**[1,5]

[1]Center for Heart Failure Research, Department of Medicine, University of Alabama, Birmingham, AL, Birmingham

[2]Department of Physiology and Biophysics, University of Alabama, Birmingham, AL, Birmingham

[3]Auburn University College of Veterinary Medicine, Auburn, AL

[4]School of Engineering, Auburn, AL

[5]Department of Veteran Affairs, Auburn, AL

Abstract

Background—The volume overload of isolated mitral regurgitation (MR) in the dog results in left ventricular (LV) dilatation and interstitial collagen loss. To better understand the mechanism of collagen loss we performed a gene array and overlaid regulated genes into Ingenuity Pathway Analysis (IPA).

Methods and Results—Gene arrays from LV tissue were compared in 4 dogs prior to and 4 months after MR. Cine-magnetic resonance-derived LV end-diastolic volume increased 2-fold ($p=0.005$) and LV ejection fraction increased from 41 to 53% ($p < 0.001$). LV interstitial collagen decreased 40% ($p<0.05$) compared to controls and replacement collagen was in short strands and in disarray. IPA identified Marfan's syndrome, aneurysm formation, LV dilatation, and myocardial infarction, all of which have extracellular matrix (ECM) protein defects and/or degradation. MMP-1 and -9 mRNA increased 5- ($p=0.01$) and 10-fold (0.003), while collagen I did not change and collagen III mRNA increased 1.5-fold ($p=0.02$). However, noncollagen genes important in ECM structure were significantly downregulated, including decorin, fibulin 1, and fibrillin 1. Decorin mRNA downregulation correlated with LV dilatation ($r= 0.83$ $p<0.05$). In addition, connective tissue growth factor and plasminogen activator inhibitor were downregulated, along with multiple genes in TGF-β signaling pathway, resulting decreased LV TGF-β1 activity ($p=0.03$).

Conclusions—LV collagen loss in isolated, compensated MR is chiefly due to post-translational processing and degradation. The downregulation of multiple noncollagen genes important in global ECM structure, coupled with decreased expression of multiple profibrotic factors, explain the failure to replace interstitial collagen in the MR heart.

Keywords

mitral regurgitation; gene array; TGF-β; extracellular matrix; left ventricle

Address reprints: Louis J Dell'Italia, MD, UAB Center for Heart Failure Research, Division of Cardiology, 434 BMR2, 1530 3rd Avenue South, Birmingham, AL 35294-2180, Telephone: (205) 934-3969, Fax: (205) 996-2586, loudell@uab.edu.

Disclosures: None

Introduction

The extracellular matrix (ECM) is a heterogeneous amalgam of macromolecules that are capable of self-assembly into a multimeric structure that contribute to the scaffolding of cells in the heart. In addition to collagen, the multimeric structure contains molecules that stabilize collagen and contribute to integrity of the entire ECM by connecting individual cardiomyocytes and cardiomyocyte bundles in a laminar structure. This structural organization maintains ventricular shape and provides for transmission of forces during systole across the myocardial wall.[1] An intact ECM is maintained in pressure overload. However, over time pressure overload produces concentric LV and cardiomyocyte hypertrophy and LV fibrosis.[2] In contrast, the volume overload of isolated MR in the dog produces eccentric LV remodeling, which is characterized by LV dilation and wall thinning, cardiomyoctye elongation, and a decrease in interstitial collagen.[3–5] We have shown that interstitial collagen loss within 12 hours after the volume overload of aortocaval fistula in the rat causes LV dilatation. This precedes cardiomyoctye elongation, suggesting that collagen breakdown is the first step in the pathophysiology of LV dilatation in response to a pure volume overload.[6]

Evidence from our dog model of isolated MR suggests that persistent loss of interstitial collagen is central to chronic eccentric LV and cardiomyocyte remodeling, but the molecular basis remains unclear. This is an important question because there is currently no recommended medical therapy to attenuate LV remodeling and thereby delay the need for valve surgery in patients with isolated MR.[7] Chronic angiotensin-converting enzyme (ACE) inhibition[5,8] and angiotensin II (Ang II) receptor (AT_1 receptor) blockade,[9] which reduce cardiomyocyte remodeling and collagen accumulation in pressure overload, do not attenuate LV dilatation, cardiomyocyte elongation, and interstitial collagen loss in the dog model of isolated MR. This illustrates that concentric remodeling in pressure overload and eccentric remodeling in isolated MR have different underlying mechanisms of ECM turnover and synthesis.

We have shown that eccentric LV remodeling in isolated, compensated MR is associated with increased matrix metalloproteinase (MMP) activity, loss of interstitial collagen and cardiomyocyte elongation.[4,5] Animal models of aortocaval fistula in the rat and pacing tachycardia in the pig have shown that MMP inhibition significantly attenuates LV dilatation by preventing interstitial collagen loss, implicating collagen degradation in the pathophysiology of LV remodeling and heart failure.[10,11] Here, we report a more global defect of ECM homeostasis. Using gene array, we not only found marked increases in MMP gene expression but also significant decreases in the expression of critical noncollagen ECM scafolding protein and glycoprotein genes, as well as a decreased expression of multiple profibrotic growth factors in the LV myocardium of dogs with LV chronic isolated MR.

Methods

Creation of Mitral Regurgitation

Mitral valve regurgitation was induced at Auburn University College of Veterinary Medicine in conditioned mongrel dogs of either sex (19–26 Kg) by chordal rupture as previously described in our laboratory.[3–5,9] Magnetic resonance imaging and LV hemodynamics were performed in all dogs prior to MR induction and after 4 months of MR under isofluorane anesthesia. Biopsy tissue was taken from the LVs of each dog prior to induction of MR. Animals were transported to the University of Alabama at Birmingham (UAB) for the terminal experiments. This study was approved by the Animal Resource Programs at UAB and Auburn University College of Veterinary Medicine.

Magnetic Resonance Imaging

Dogs were anesthetized with isofluorane anesthesia and cine-magnetic resonance imaging was performed with a Picker Vista 1.0T magnet. Endocardial and epicardial contours were manually traced on the LV end-diastolic (ED) and end-systolic (ES) images. The contours were traced to exclude the papillary muscles. LVED and LVES volumes were determined by summating serial short axis slices as previously described in our laboratory.[3,5]

Sacrifice Study

Dogs were maintained under a deep plane of isofluorane anesthesia and were mechanically ventilated (Harvard Apparatus, Inc., MA). The heart was arrested with KCl and quickly extirpated, placed in phosphate buffered ice slush, and the coronaries flushed with ice-cold Krebs solution (118mM NaCl, 27.1mM $NaHCO_3$, 1.0mM KH_2PO_4, 1.2mM $MgSO_4.7H_2O$, 11.1mM glucose, 11.3mM HEPES). The LV was cut into pieces that were either perfusion fixed with 3% paraformaldehyde, snap frozen in liquid nitrogen, or placed in an RNA stabilizing solution (RNA later – Qiagen Sciences, MD) for subsequent analyses.

RNA Isolation

Total RNA was extracted from LV prior to MR induction and at 4 months of MR using Qiagen RNeasy Fibrous Tissue Mini Kit (Qiagen Sciences, MD). DNase I (Qiagen Sciences, MD) was applied to remove genomic contamination. Negative RT-PCR using GAPDH primers (F: 5'gaa cat cat ccc tgc ttc cac 3', R: 5'acc acc tgg tcc tca gtg ta3') ensured no genomic contamination. Integrity of the RNA was evaluated on the BioRad Experion (Bio-Rad Laboratories, CA). Samples with OD ratio 260/280 >1.8, 28S/18S >1.5 were selected for microarray processing.

Microarray Analysis

Two color microarrays were performed on Agilent 4×44 canine array chips with 42,000+ predicted *C. familiari* genes following established Agilent 2-color protocol (Agilent Technologies, CA). Comparative analysis between expression profiles for Agilent experiments was carried out using Genespring GX 7.3.1 (Agilent Technologies, CA). The data was normalized using Agilent 2 color scenario. Gene expression data was normalized in two ways: 'per chip normalization' and 'per gene normalization'. For 'per chip normalization', all expression data on a chip is normalized to the 50^{th} percentile of all values on that chip. For 'per gene normalization' all expression data on a chip is normalized to the median expression level of that gene across all samples. Dye swap hybridizations were merged with their counterparts, with the average of the two values (one of them inverted to account for the dye swap) for a spot taken as the representative value. A gene list was generated containing 24,196 gene sequence flagged as present. The "Present" list was then filtered using "Filter by expression", "Self confidence" and "Benjamini and Hochberg false discovery test". Significant genes were selected with a cut-off of $p < 0.05$ and fold change > 1.5.

Ingenuity Pathway Analysis (IPA)

The selected genes were subsequently analyzed using IPA 5.0 (Ingenuity Systems Inc., CA). Functions and pathways, which were predicted to be influenced by the differentially expressed genes, were ranked in order of significance and further analyzed by overlaying with cardiovascular function and disease.

Verification of Gene Expression Using Real-Time RT-PCR

Quantitative real-time PCR was performed using Bio-RAD iCycler iQ™ system (Bio-Rad Laboratories, CA) on 500 ng total RNA from microarray samples to verify array data.

Selected genes and primer sequences (Sigma-Genosys, Woodlands, TX) are presented in Table 1. GAPDH was chosen as an endogenous control.

Western Blot for Decorin, TGF-β receptor 2 and Phospho-smad2

100 mg tissue from LV endocardium of normal and 4-month MR dogs were homogenized in 1.5 ml RIPA buffer (Sigma-Aldrich, MO) containing the appropriate protease and phosphatase inhibitor (Roche Diagnostics, Mannheim, Germany). 40 μg total proteins from each sample were subjected to SDS-polyacrylamide gel electrophoresis followed by western blot analysis. Primary antibodies used were decorin (H-80) (Santa Cruz Biotechnology, Inc, CA), TGF-β receptor 2 (C-16) (Santa Cruz Biotechnology, Inc, CA) and phosphosmad 2 (Ser465/467) (Upstate Cell Signaling Solutions, NY) respectively. Membranes were stripped and reblotted with anti-tubulin (Sigma-Aldrich, MO) for endogenous control.

TGF- β1 Activity

60~100 mg LV endo- and epicardium were homogenized in PBS (pH 7.4) containing complete protease inhibitor (Roche Diagnostics, Mannheim, Germany) and centrifuged at 12,000 g for 10 minutes. Total protein in the supernatant was measured with a Bradford protein assay kit (Bio-Rad Laboratories, CA). TGF-β1 activity was determined by commercial ELISA kit (R&D Systems, MN). TGF- β 1 activity was expressed per mg of protein in each sample.

Total Collagen Analysis

LV endocardium total collagen was determined by hydroxyproline method according to previously described colormetric method.[12] Morphological evaluation of volume percent collagen was performed on tissues from normal dogs and 4 month MR dogs by Picric Acid Sirius Red (PASR) as previous described in our lab.[13]

Statistical Analysis

Data are presented as mean ± SEM. Comparison within groups (magnetic resonance LV volumes) was tested by paired t-test (RT-PCR) or non paired t-test between control and MR dogs (western blot, collagen analysis). A p value of < 0.05 was considered statistically significant.

Results

Morphometry, Magnetic Resonance Imaging and Hemodynamics

LV mass to body ratio increased in MR vs normal dogs (3.9 ± 0.2 to 4.9 ± 0.3 g/kg, $p = 0.04$). Total LV endocardial collagen by hydroxyproline was decreased 35% ($p < 0.05$) and interstitial collagen volume fraction decreased 40% ($p < 0.05$) in four month MR dogs vs. normal dog (Fig.1). In MR dogs, LVEDV increased from 34 ± 4 to 64 ± 9 ml ($p < 0.005$) as LVESV increased from 20 ± 4 to 31 ± 8 ml ($p=0.03$), resulting in a three-fold increase in stroke volume (13 ± 1 to 33 ± 2 ml, $p < 0.006$). Cardiac output decreased from 4.14 ± 0.56 to 3.14 ± 0.44 liters/min ($p < 0.005$) as LVES pressure remained unchanged from baseline. LVED pressure increased from 10 ± 2 to 19 ± 3 mmHg ($p < 0.03$) and LV ± dP/dt_{max} did not change; however, LV ejection fraction increased from 41 ± 5 to 53 ± 6% ($p < 0.007$) after four months of MR (Tables 2 and 3).

Microarray Analysis

659 genes were differently expressed by at least 1.5 fold in MR dogs ($p < 0.05$), including 217 upregulated and 442 downregulated genes. The heat map in Figure 2 demonstrates a consistent pattern of change of these genes in the four MR dogs. Table 4 lists genes well

established in the pathophysiology of cardiovascular disease. Figure 3 A lists noncollagen ECM genes that are down-regulated > 1.5 fold. These include microfibrillar genes fibrilin 1 and fibulin 1, and glycoprotein genes including multimerin, vitronectin, decorin, versican, and lumican. In addition, there is significant downregulation of integrin α-V. Plasminogen activator inhibitor type 1 (PAI-1), thrombospondin 1, TGF-β receptor 2, TGF-β receptor 3, connective tissue growth factor (CTGF) are significantly downregulated, while MMP-1and MMP-9 are increased 5- and 10-fold, respectively (Fig. 3B).

Validation of Microarray with Quantitative PCR

Quantitative PCR validated microarray results for vonwillibrand factor (VWF), TGF-βR2, TGF-βR3, fibullin-1, lumican, fibrillin 1, decorin, PAI-1, KITLG, MMP-1, and MMP-9. There was excellent agreement between microarray and quantitative PCR (Fig. 4A), which was documented by linear regression analysis ($R^2 = 0.98$, $p < 0.01$, Fig. 4B).

Clustering Gene Expression Patterns

The 659 genes canine genes which changed > 1.5 fold were matched to the human ID according to their sequence identity and 322 genes were mapped in IPA, resulting in a network score of 52 for dermatological diseases. Genes in this network collectively define an association between ECM loss and edema in skin diseases, such as bullous pemphigoid. Overlaying this network with cardiovascular function and disease identified Marfan's syndrome, aneurysm formation, LV dilatation, vascular injury and myocardial infarction, all of which are characterized by ECM protein defects and/or degradation (Fig. 5).

Quantification of Decorin Protein and TGF-β1 Activity

The fold-decrease in decorin mRNA correlated with the fold-increase in LVEDD with MR (Fig. 6), as LV endocardial decorin protein in MR demonstrated a strong trend to decrease vs. normal dogs ($p = 0.08$). Protein expression of TGF-β receptor 2 (Fig. 7A), phosphosmad 2 and TGF-β1 activity were significantly decreased in MR vs. normal dogs ($P < 0.05$) (Fig. 7B and C).

Discussion

Left ventricular dilatation and remodeling has been associated with a breakdown of interstitial collagen and increased expression and activation of MMPs in models of heart failure[10,11] and in isolated MR.[3–5] Here, for the first time, we report a global defect in the ECM with downregulation of multiple noncollagen microfibillar and glycoprotein genes essential to collagen assembly and total ECM structure. Further, in the face of increased expression of MMP genes, there is decreased expression of growth factor genes that control synthesis of these ECM components. This could explain the failure of orderly replacement of interstitial collagen, resulting in cardiomyocyte and myofiber slippage and adverse eccentric LV remodeling in isolated MR.

We chose the four month stage of MR because there is two-fold increase in LVED volume but an increase in LV ejection fraction. Thus, the LV is in a relatively compensated state and not in overt failure. IPA identified Marfan's syndrome, Ehrlos Danlos syndrome, aneurysm formation, myocardial infarction, and LV dilatation (Fig. 5). All of these disorders are marked by ECM protein defects and/or ECM degradation. Indeed, MMP-1 and -9 are highly upregulated and occupy a central location in the IPA map in Figure 5; however, there is also a striking downregulation of multiple essential noncollagen ECM genes (Table 4). Of these genes, decorin is the most abundant in the normal heart and is associated with all major type collagens[14] (Fig.3A). It co-localizes with large helical collagen fibers[15] and binds specific sites on collagen molecules as they assemble, thereby increasing the tensile strength of

uncross-linked collagen fibers.[16] Decorin null mice have more severe LV dilation after experimentally-induced myocardial infarction.[17] In MR dogs, decorin mRNA downregulation correlated with the increase in LVEDD (Fig. 6B). Collagen I mRNA was unchanged and collagen IIIα1 mRNA was increased 1.5-fold, while total collagen was decreased by 30%, suggesting a post-translational degradation. Analysis of collagen showed diffuse endomysial collagen loss with only short strands randomly distributed in the LV (Fig. 1). It is tempting to speculate that decreased decorin resulted in a less stable collagen making it more prone to degradation, which is identified as a direct interaction of MMP-9 on decorin by IPA in Figure 5.

The ECM is made of a collection of noncollagen microfibrils and glycoproteins that serve to connect collagen to cell surfaces and promote cell–cell interactions. Fibrillin 1 is the major component of extracellular microfibrils that are distributed throughout perivascular and perimysial areas.[18] Fibrillin-1 gene mutations are responsible for Marfan's syndrome,[19] while fibulins are implicated in elastic matrix fiber assembly, structural integrity and function.[20] Multimerin,[21] versican,[22] lumican,[23] and vitronectin[24] are important ECM glyocproteins that are also downregulated in the MR heart. These molecules link microfibrils, such as fibrillin, elastic fibers and collagen to cell surfaces, as is indicated by adhesion of fibronectin matrix to versican defects in the IPA map.

It is of note that integrin α_5 is also downregulated. Integrins mechanically link the cytoskeleton to the ECM in cardiomyocytes and are important in transducing mechanical signals to the cardiomyocyte. Integrins, incuding α_5-integrin, as well as phosphorylation of focal adhesion kinase (FAK) have been shown to be upregulated in pressure overload.[25] In four week MR dogs, we found a decrease in FAK tyrosine phosphorylation along with FAK interaction with adapter and cytoskeletal proteins, p130*Cas* and paxillin.[26] In contrast, FAK phoshporlyation is upregulated in pressure overload and its silencing attenuates the increase in collagen content and fibrosis in response to pressure overload.[27] In addition, IPA identified downregulation of epidermoid growth factor receptor (EGFR). EGFR stimulation triggers a cascade of events that affect cell morphology, FAK phosphorylation, as well as phosphorylation of many cytoskeletal proteins and has been associated with growth and aggressiveness of tumors.[28] A loss of ECM and its signals to the cell surface could result in decreased integrin and EGFR expression in MR.

Central to the decrease in ECM component synthesis is the downregulation of the group complex of TGF-β and of CTGF, which are both increased in models of pressure overload.[29] TGF-β regulates decorin, fibulin and fibrillin production[30,31] and downregulation of the TGF-β group complex was verified by significant decreases in phosphorylated smad 2 and TGF-β1 activity in the MR LVs. CTGF mediates interactions with growth factors, integrins and ECM components and is required for ECM production. In the CTGF knockout mouse, there is a decrease in chondrocyte proliferation, tensile strength of cartilage, and growth plate angiogenesis.[32] CTGF also mediates TGF-β fibrotic responses by suppression of Smad7 transcription[33] and binding of CTGF to TGF-β enhances TGF-β1 activity.[34] Finally, there is a three-fold decrease in PAI-1 expression, a principal inhibitor of plasminogen activators (PAs) that promotes fibrosis by preventing MMP activation and ECM degradation by PAs and plasmin.[35] PAI-1 is upregulated markedly early in the course of pressure overload in the mouse heart.[36] Thus, IPA identified downregulation of multiple growth factors that are central to ECM integrity.

IPA also identified marked upregulation of the chemokine proplatelet basic protein (CXCL7),[37] adhesion molecules selectin L and selectin P, and stem cell factor KITLG, resulting in links to vascular injury, myocardial infarction, and degranulation of granulocytes and mast cells (Fig. 5). This imflammatory feature is consistent with our

finding of early and persistent increase in mast cells and chymase activity in the MR dog.[4] Mast cells contain a collection of cytokines and proteolytic enzymes, including tryptase and chymase, which activate MMPs.[38] Indeed, mast cell tumors in dogs have increased MMP-2 and -9 activity that predicts tumor invasion and histological score.[39] In the volume overload of aortocaval fistula in the rat, mast cell stabilization attenuates LV dilatation, presumably by inhibiting MMP activation.[40] Thus, influx of mast cells and other inflammatory cells could be responsible for the increase in MMPs as well as their activation via their inflammatory cell proteases, but the increase in MMP mRNA also suggests production from resident cardiac cells such as fibroblasts.

We also found an increase in factors that have antifibrotic effects on fibroblasts phospholipase A2 (PLA2) and prostaglandin E2 (PGE2) receptor, as well as down-regulation of 3', 5'-cyclic GMP specific phosphodiesterase PDE5, and PDE9. PGE2, a product of PLA2, causes anti-fibrotic effects by increasing MMP-1 activity, decreasing fibroblast collagen synthesis via bradykinin and nitric oxide, and stimulating brain natriuretic peptide expression.[41] Finally, downregulation of PDE5 increases cyclic GMP and has an antifibrotic effect on cardiac fibroblasts.[42] Recently, it was shown that PDE5 inhibition prevented fibrosis in pressure overload in the mouse.[43] We speculate that the increased adrenergic drive in the dog with isolated MR[13] plays a major role in the downregulation of PDEs, contributing to decreased ECM synthesis.

Isolated MR is a unique form of volume overload in which the excess volume is ejected into the low pressure left atrium. This study supports the contention that this low pressure type of volume overload induces molecular signals not only for increased MMPs but also for decreased synthesis of noncollagen ECM proteins and their growth factors. Although this may initially allow for a more compliant LV chamber, over time persistent ECM loss leads to myocyte slippage, apoptosis[44] and cardiomyocyte dysfunction. Taken together, molecular signals that decrease synthesis in the face of increased degradation of ECM could explain why antifibrotic drugs such as ACE inhibitors AT_1 receptor blockers do not attenuate LV dilatation and ECM loss in the canine model of isolated MR. These findings call for a new treatment paradigm that addresses ECM loss to attenuate progressive LV dilatation in isolated MR.

Acknowledgments

Funding Source: This study is supported by Department of Veteran Affairs (LJD) and National Heart, Lung and Blood Institute SCCOR in Cardiac Dysfunction P50HL077100.

References

1. LeGrice IJ, Smaill BH, Chai LZ, Edgar SG, Gavin JB, Hunter PJ. Laminar structure of the heart: ventricular myocyte arrangement and connective tissue architecture in the dog. Am J Physiol. 1995; 269:H571–H582. [PubMed: 7653621]
2. Sasayama S, Ross J Jr, Franklin D, Bloor CM, Bishop S, Dilley RB. Adaptations of the left ventricle to chronic pressure overload. Circ Res. 1976; 38:172–178. [PubMed: 129304]
3. Dell'Italia LJ, Meng QC, Balcells E, Straeter-Knowlen IM, Hankes GH, Dillon R, Cartee RE, Orr R, Bishop SP, Oparil S, et al. Increased ACE and chymase-like activity in cardiac tissue of dogs with chronic mitral regurgitation. Am J Physiol. 1995; 269:H2065–H2073. [PubMed: 8594918]
4. Stewart JA Jr, Wei CC, Brower GL, Rynders PE, Hankes GH, Dillon AR, Lucchesi PA, Janicki JS, Dell'Italia LJ. Cardiac mast cell- and chymase-mediated matrix metalloproteinase activity and left ventricular remodeling in mitral regurgitation in the dog. J Mol Cell Cardiol. 2003; 35:311–319. [PubMed: 12676546]

5. Dell'italia LJ, Balcells E, Meng QC, Su X, Schultz D, Bishop SP, Machida N, Straeter-Knowlen IM, Hankes GH, Dillon R, Cartee RE, Oparil S. Volume-overload cardiac hypertrophy is unaffected by ACE inhibitor treatment in dogs. Am J Physiol. 1997; 273:H961–H970. [PubMed: 9277516]
6. Ryan TD, Rothstein EC, Aban I, Tallaj JA, Husain A, Lucchesi PA, Dell'Italia LJ. Left ventricular eccentric remodeling and matrix loss are mediated by bradykinin and precede cardiomyocyte elongation in rats with volume overload. J Am Coll Cardiol. 2007; 49:811–821. [PubMed: 17306712]
7. Borer JS, Bonow RO. Contemporary approach to aortic and mitral regurgitation. Circulation. 2003; 108:2432–2438. [PubMed: 14623790]
8. Nemoto S, Hamawaki M, De Freitas G, Carabello BA. Differential effects of the angiotensin-converting enzyme inhibitor lisinopril versus the beta-adrenergic receptor blocker atenolol on hemodynamics and left ventricular contractile function in experimental mitral regurgitation. J Am Coll Cardiol. 2002; 40:149–154. [PubMed: 12103269]
9. Perry GJ, Wei CC, Hankes GH, Dillon SR, Rynders P, Mukherjee R, Spinale FG, Dell'Italia LJ. Angiotensin II receptor blockade does not improve left ventricular function and remodeling in subacute mitral regurgitation in the dog. J Am Coll Cardiol. 2002; 39:1374–1379. [PubMed: 11955858]
10. Chancey AL, Brower GL, Peterson JT, Janicki JS. Effects of matrix metalloproteinase inhibition on ventricular remodeling due to volume overload. Circulation. 2002; 105:1983–1988. [PubMed: 11997287]
11. Spinale FG, Coker ML, Krombach SR, Mukherjee R, Hallak H, Houck WV, Clair MJ, Kribbs SB, Johnson LL, Peterson JT, Zile MR. Matrix metalloproteinase inhibition during the development of congestive heart failure: effects on left ventricular dimensions and function. Circ Res. 1999; 85:364–376. [PubMed: 10455065]
12. Edwards CA, O'Brien WD Jr. Modified assay for determination of hydroxyproline in a tissue hydrolyzate. Clin Chim Acta. 1980; 104:161–167. [PubMed: 7389130]
13. Tallaj J, Wei CC, Hankes GH, Holland M, Rynders P, Dillon AR, Ardell JL, Armour JA, Lucchesi PA, Dell'Italia LJ. Beta1-adrenergic receptor blockade attenuates angiotensin II-mediated catecholamine release into the cardiac interstitium in mitral regurgitation. Circulation. 2003; 108:225–230. [PubMed: 12847066]
14. Bianco P, Fisher LW, Young MF, Termine JD, Robey PG. Expression and localization of the two small proteoglycans biglycan and decorin in developing human skeletal and non-skeletal tissues. J Histochem Cytochem. 1990; 38:1549–1563. [PubMed: 2212616]
15. Thieszen SL, Rosenquist TH. Expression of collagens and decorin during aortic arch artery development: implications for matrix pattern formation. Matrix Biol. 1995; 14:573–582. [PubMed: 8535607]
16. Sini P, Denti A, Tira ME, Balduini C. Role of decorin on in vitro fibrillogenesis of type I collagen. Glycoconj J. 1997; 14:871–874. [PubMed: 9511994]
17. Weis SM, Zimmerman SD, Shah M, Covell JW, Omens JH, Ross J Jr, Dalton N, Jones Y, Reed CC, Iozzo RV, McCulloch AD. A role for decorin in the remodeling of myocardial infarction. Matrix Biol. 2005; 24:313–324. [PubMed: 15949932]
18. Bouzeghrane F, Reinhardt DP, Reudelhuber TL, Thibault G. Enhanced expression of fibrillin-1, a constituent of the myocardial extracellular matrix in fibrosis. Am J Physiol Heart Circ Physiol. 2005; 289:H982–H991. [PubMed: 15849235]
19. Mellody KT, Freeman LJ, Baldock C, Jowitt TA, Siegler V, Raynal BD, Cain SA, Wess TJ, Shuttleworth CA, Kielty CM. Marfan syndrome-causing mutations in fibrillin-1 result in gross morphological alterations and highlight the structural importance of the second hybrid domain. J Biol Chem. 2006; 281:31854–31862. [PubMed: 16905551]
20. Argraves WS, Greene LM, Cooley MA, Gallagher WM. Fibulins: physiological and disease perspectives. EMBO Rep. 2003; 4:1127–1131. [PubMed: 14647206]
21. Doliana R, Canton A, Buciotti F, Mongiat M, Bonalodo P, Colombatti A. Structure, chromosomal localization, and promoter analysis of the human elastin microfibril interfase located protein (EMILIN) gene. J Biol Chem. 2000; 275:785–792. [PubMed: 10625608]

22. Wight TN, Merrilees MJ. Proteoglycans in atherosclerosis and restenosis: key roles for versican. Circ Res. 2004; 94:1158–1167. [PubMed: 15142969]
23. Ying S, Shiraishi A, Kao C, Converse RL, Funderburgh JL, Swiergiel J, Roth MR, Conrad GW, Kao W. Characterization and expression of the mouse lumican gene. J Biol Chem. 1997; 272:30306–30313. [PubMed: 9374517]
24. Gebb C, Hayman EG, Engvall E, Ruoslahti E. Interaction of vitronectin with collagen. J Biol Chem. 1986; 261:16698–16703. [PubMed: 2430969]
25. Babbit CJ, Shai S-Y, Harpf AE, Pham CG, Ross RS. Modulation of integrins and integrin signaling molecules in the pressure overloaded murine ventricle. Histochem Cell Biol. 2002; 418:431–439.
26. Sabri A, Rafio K, Kolpakov MA, Dillon R, Dell'Italia JL. Impaired focal adhension signaling early in the course of volume overload due to mitral regurgitation in the dog. Effect of beta 1 adrenergic receptor blockade. Circ Res. 2008
27. Clemente CFMZ, Tornatore TF, Theizen TH, Deckmann AC, Pereira TV, Lopes-Cendes I, Souza JRM, Franchini KG. Targeting focal adhesion kinase with small interfering RNA prevents and reverses load-induced cardiac hypertrophy in mice. Circ Res. 2007; 101:1339–1348. [PubMed: 17947798]
28. Nelson JM, Fry DW. Cytoskeletal and morphological changes associated with the specific suppression of the epidermal growth factor receptor tyrosine kinase activity in A431 human epidermoid carcinoma. Ex Cell Res. 1997; 233:383–390.
29. Zhang YM, Bo J, Taffet GE, Chang J, Shi J, Reddy AK, Michael LH, Schneider MD, Entman ML, Schwartz RJ, Wei L. Targeted deletion of ROCK1 protects the heart against pressure overload by inhibiting reactive fibrosis. Faseb J. 2006; 20:916–925. [PubMed: 16675849]
30. Heimer R, Bashey RI, Kyle J, Jimenez SA. TGF-beta modulates the synthesis of proteoglycans by myocardial fibroblasts in culture. J Mol Cell Cardiol. 1995; 27:2191–2198. [PubMed: 8576935]
31. Rosenkranz S. TGF-β_1 and angiotensin networking in cardiac remodeling. Cardiovasc Res. 2004; 63 423-422.
32. Ivkovic S, Yoon BS, Popoff SN, Safadi FF, Libuda DE, Stephenson RC, Daluiski A, Lyons KM. Connective tissue growth factor coordinates chondrogenesis and angiogenesis during skeletal development. Development. 2003; 130:2779–2791. [PubMed: 12736220]
33. Wahab NA, Weston BS, Mason RM. Modulation of the TGFbeta/Smad signaling pathway in mesangial cells by CTGF/CCN2. Exp Cell Res. 2005; 307:305–314. [PubMed: 15950619]
34. Abreu JG, Ketpura NI, Reversade B, De Robertis EM. Connective-tissue growth factor (CTGF) modulates cell signalling by BMP and TGF-beta. Nat Cell Biol. 2002; 4:599–604. [PubMed: 12134160]
35. Loskutoff DJ, Quigley JP. PAI-1, fibrosis, and the elusive provisional fibrin matrix. J Clin Invest. 2000; 106:1441–1443. [PubMed: 11120750]
36. Bloor CM, Nimmo L, McKirnan MD, Zhang Y, White FC. Increased gene expression of plasminogen activators and inhibitors in left ventricular hypertrophy. Mol Cell Biochem. 1997; 176:265–271. [PubMed: 9406171]
37. Baggiolini M. Chemokines and leukocyte traffic. Nature. 1998; 392:565–568. [PubMed: 9560152]
38. Caughey GH. Mast cell tryptases and chymases in inflammation and host defense. Immunol Rev. 2007; 217:141–154. [PubMed: 17498057]
39. Leibman NF, Lana SE, Hansen RA, Powers BE, Fettman MJ, Withrow SJ, Ogilvie GK. Identification of matrix metalloproteinases in canine cutaneous mast cell tumors. J Vet Intern Med. 2000; 14:583–586. [PubMed: 11110378]
40. Brower GL, Chancey AL, Thanigaraj S, Matsubara BB, Janicki JS. Cause and effect relationship between myocardial mast cell number and matrix metalloproteinase activity. Am J Physiol. 2002; 283:H518–H525.
41. Qian JY, Leung A, Harding P, LaPointe MC. PGE2 stimulates human brain natriuretic peptide expression via EP4 and p42/44 MAPK. Am J Physiol. 2006; 290:H1740–H1746.
42. Zahabi A, Picard S, Fortin N, Reudelhuber TL, Deschepper CF. Expression of constitutively active guanylate cyclase in cardiomyocytes inhibits the hypertrophic effects of isoproterenol and aortic constriction on mouse hearts. J Biol Chem. 2003; 278:47694–47699. [PubMed: 14500707]

43. Takimoto E, Champion HC, Li M, Belardi D, Ren S, Rodriguez ER, Bedja D, Gabrielson KL, Wang Y, Kass DA. Chronic inhibition of cyclic GMP phosphodiesterase 5A prevents and reverses cardiac hypertrophy. Nat Med. 2005; 11:214–222. [PubMed: 15665834]

44. Michel JB. Anoikis in the cardiovascular system: known and unknown extracellular mediators. Arterioscler Thromb Vasc Biol. 2003; 23:2146–2154. [PubMed: 14551156]

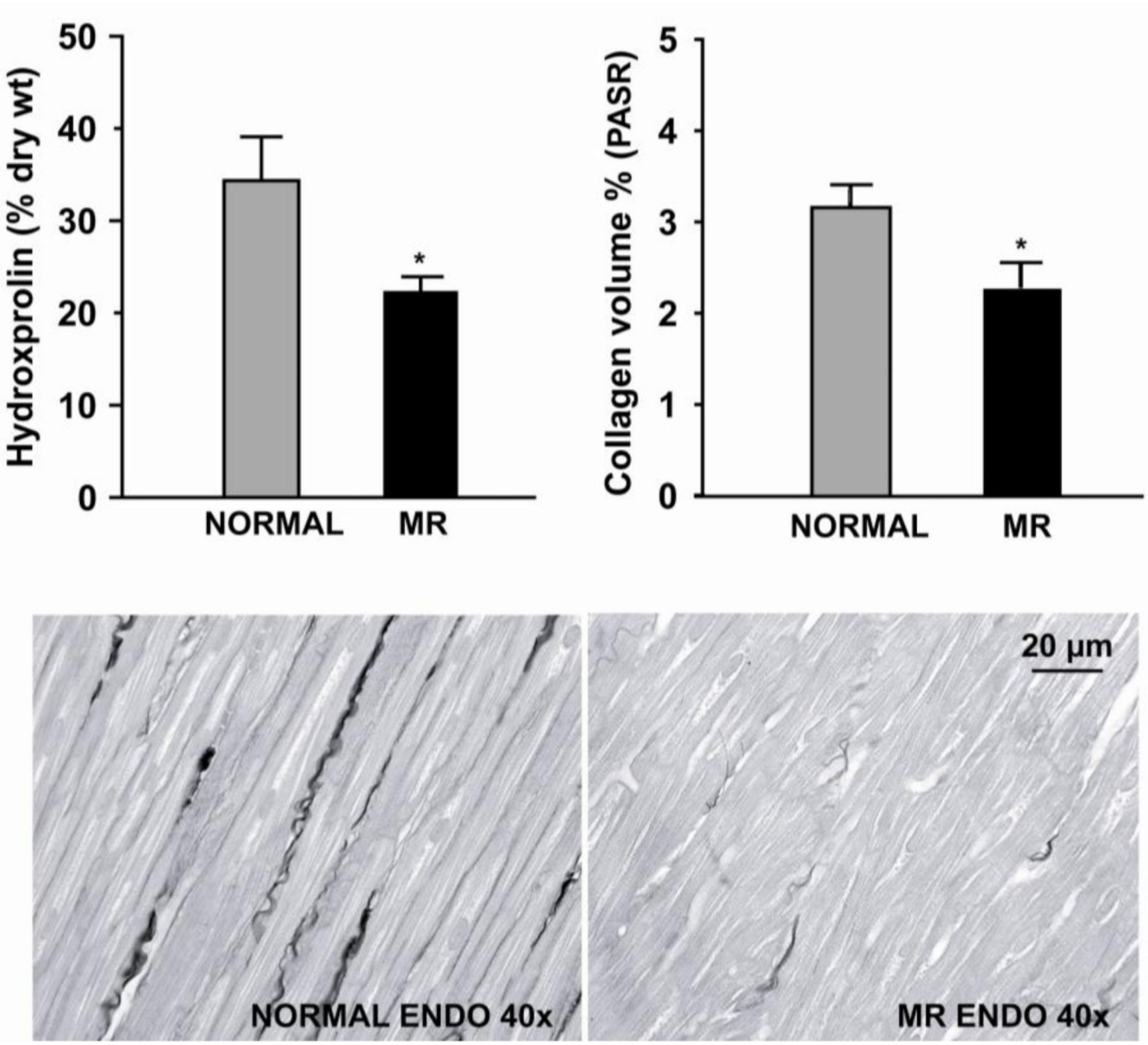

Figure 1.
Total collagen (% dry weight tissue) in the LV of MR vs. normal dogs determined by hydroxyproline method (left) and volume percent collagen by PASR (right). Values are mean ± SE. Interstitial collagen in normal and 4 month MR dog demonstrates marked loss of interstitial collagen and randomly dispersed strands of collagen (bottom).

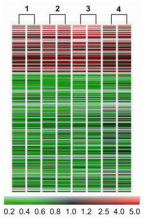

Figure 2.
Heatmap of the 659 genes altered greater than 1.5 fold ($p<0.05$) in the four MR dogs vs. baseline(1–4). Two-color gene array with dye swap was applied. Red = upregulation, black = no change, green = downregulation vs. baseline with scale of color corresponding to fold-change.

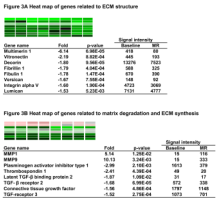

Figure 3.

Genes altered in MR related to ECM structure (A) and TGF-β pathway and ECM degradation (B).

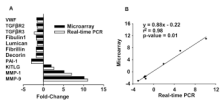

Figure 4.

Comparison of microarray and real-time RT PCR (A). Regression line between microarray and real-time RT PCR (B).

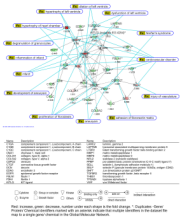

Figure 5.
Cardiovascular dysfunction and disorders identified by IPA with glossary for gene symbols in the table below.

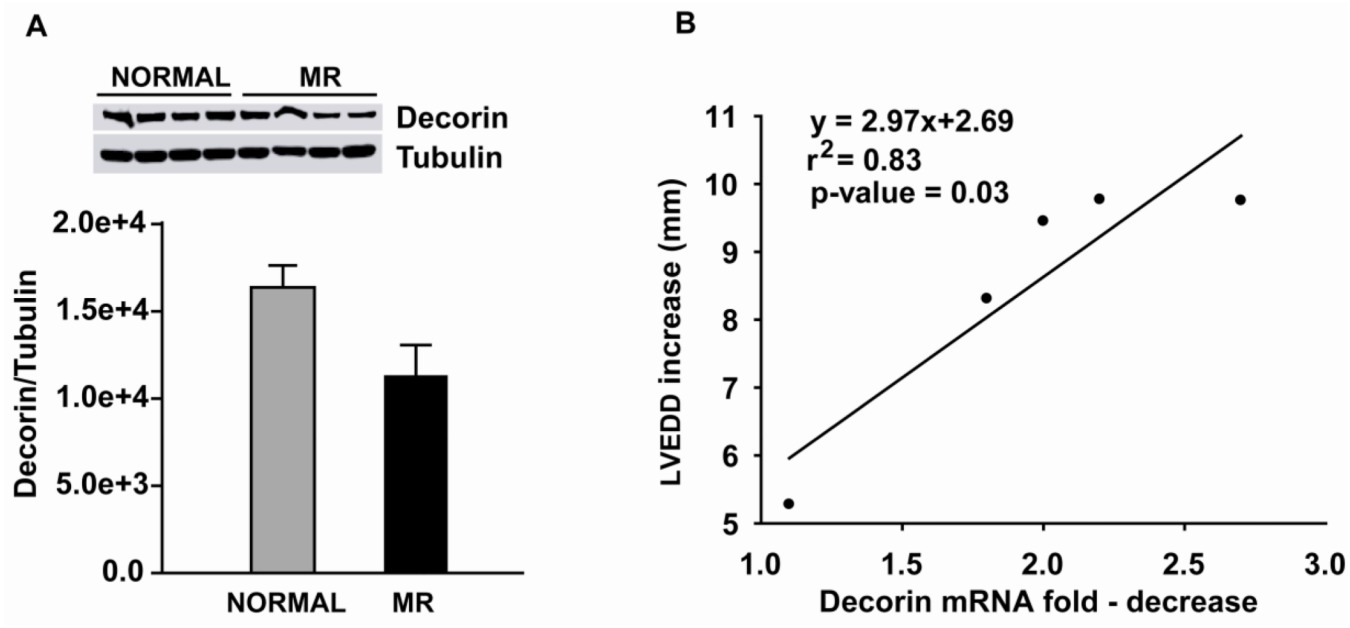

Figure 6.

Decorin protein expression in 4 month MR vs. normal dogs with corresponding western blot for normal and MR. (A). Correlation of the decrease of decorin mRNA with the increase of LVEDD in MR dogs (n=5) (B).

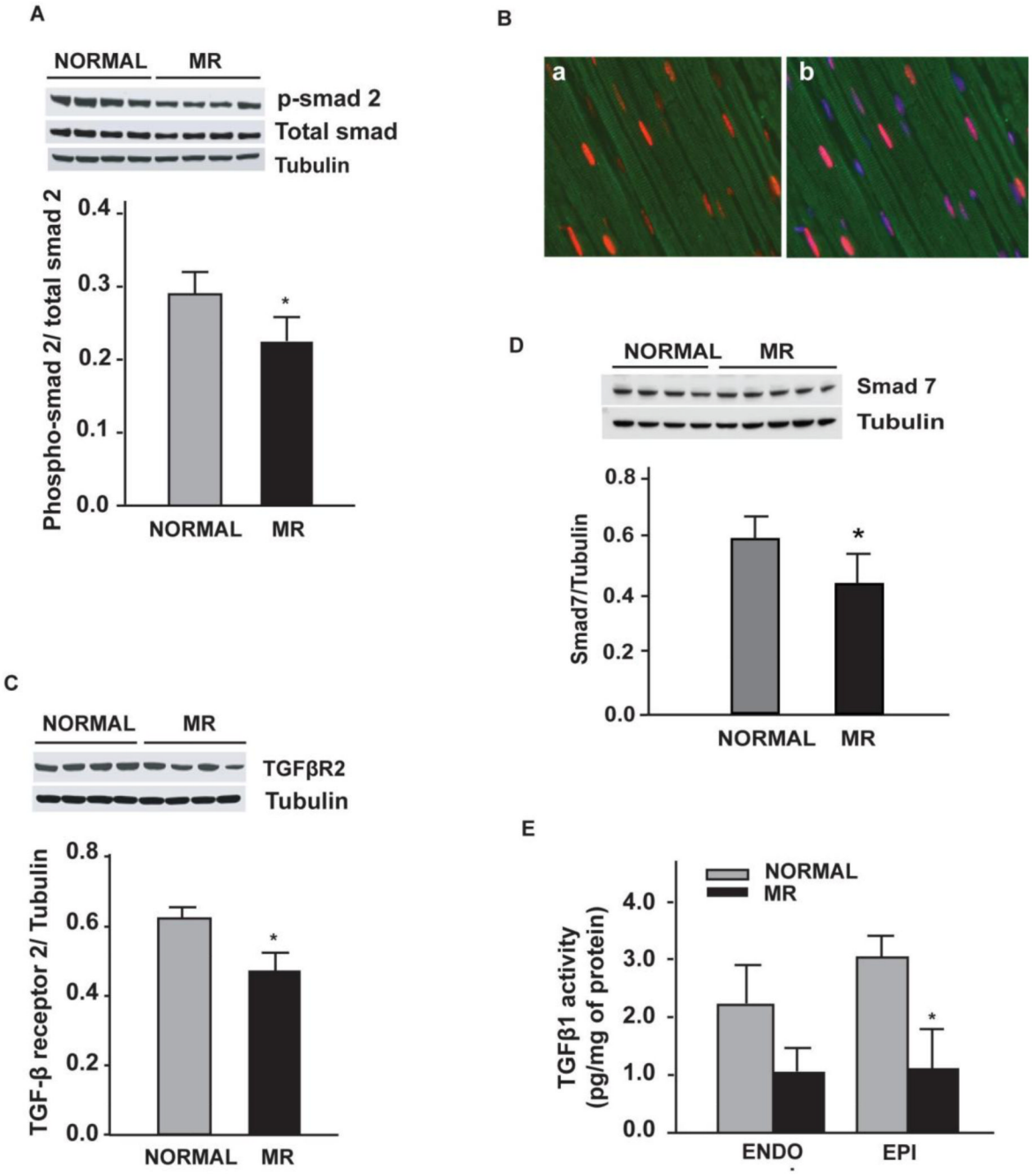

Figure 7.

Western blot of TGF-β receptor 2 in LV endocardium in normal vs MR dogs (A), phospho-smad 2 in normal vs MR dogs (B). LV tissue TGF-β activity in 4 month MR dogs vs. normal dogs (C). * = $p < 0.05$

Table 1

Primer sequences for validating microarray by real-time PCR

Gene Name	Forward Primer	Reverse Primer	Genebank ID
MMP1	5'gtgcctcctacaagatagca3'	5'cgttgattttctttaccctctgc3'	XM_849520.1
MMP9	5'ggcaaattccagacctttgag3'	5'tacacgcgagtgaaggtgag3'	NM_001003219.1
GAPDH	5'gaacatcatccctgcttccac3'	5'accacctggtcctcagtgta3'	NM_001003142.1
PAI-1	5'tcaagaggtgctgtatgtgt 3'	5'ccatgaaaaggactgttcct 3'	XM_844252.1
TGF-βR2	5'caaggccaagctgaagcagaa3'	5'tgacatgccgagtgaggtact3'	XM_534237
TGF-βR3	5'ctacctgcaaggccaagatga3'	5'tcaggtcggctgaagaaggaa3'	XM_547284.2
Lumican	5'cagatggccaaactgccttct3'	5'gttctcattgacagtcggtatg3'	XM_539716
Decorin	5'tgaaccagatgatcgtcgtaga3'	5'ggctagatgcatcaaccttggt3'	NM_001003228.1
Fibrillin	5'cttttgcaagtgtcctcctggtt3'	5'tgctctgatgggacacatctca3'	XM_535468.2
KITLG	5'agattccagagtcagtgtcacaa3'	5'ctgtccttgtgagatttggttgt3'	NM_001012735.1
VWF1	5'gtcacttctgcaaggtcaatga3'	5'atgtccacttcctcttcagact3'	NM_001002932.1
Fibulin1	5'cacagaggacaatgactgcaa3'	5' cacgttcttctggcatgtgta3'	XM_531698.2

Table 2

Magnetic resonance imaging LV volumes and function in dogs prior to and 4 month after MR

	Baseline	MR	p-value
LVEDV	34 ± 4	64 ± 9*	0.005
LVESV	20 ± 4	31 ± 8*	0.027
LVEDD	34 ± 2	42 ± 3*	0.004
LVESD	28 ± 2	32 ± 2*	0.007
Stroke Volume (mL)	13 ± 1	33 ± 2*	0.006
Ejection Fraction (%)	41 ± 5	53 ± 6*	0.007
Sample Size (N)	4	4	

Values presented as Mean ± SEM.

* $p < 0.05$

Table 3

Hemodynamic data in dogs prior to and 4 month after MR

	Baseline	MR	p-value
CO (L/min)	4.14 ± 0.56	3.14 ± 0.44*	0.005
LVEDP (mmHg)	10 ± 2	19 ± 3*	0.03
LEVSP (mmHg)	110 ± 5	107 ± 4	0.67
LV + dP/dT (mmHg/s)	2676 ± 198	2553 ± 377	0.58
LV − dP/dT (mmHg/s)	2637 ± 127	2511 ± 147	0.2
Sample Size (N)	4	4	

Values presented as Mean ± SEM.

* $p < 0.05$

Table 4

Selected cardiovascular genes changed 1.5 fold in 4 month MR vs baseline

Name	Fold	p-value	Systematic Name	Description
PPBP	13.03	5.28E-04	A_11_P0000026703	Pro-platelet basic protein (chemokine (C-X-C motif) ligand 7)
MMP-9	10.13	3.24E-03	A_11_P0000019937	Canis familiaris matrix metalloproteinase 9
SELL	6.10	1.85E-03	A_11_P0000024990	L-selectin
MMP-1	5.14	1.25E-02	A_11_P0000032626	Matrix metalloproteinase 1 precursor
SELP	3.96	5.66E-04	A_11_P0000024991	Cell adhesion molecule (GMP140)
ANF	3.74	1.57E-02	A_11_P0000040649	Atrial natriuretic factor precursor
BNP	3.68	3.86E-03	A_11_P0000031049	Natriuretic peptides B precursor
ATF3	2.58	1.72E-02	A_11_P0000033371	Cyclic-AMP-dependent transcription factor ATF-3
CNP	2.49	5.34E-05	A_11_P0000029955	Natriuretic peptide precursor C
BDNF	2.19	1.15E-02	A_11_P0000019701	Brain-derived neurotrophic factor
PDE4D	2.00	3.88E-03	A_11_P0000030852	cAMP-specific phosphodiesterase 4D
KITLG	1.93	3.36E-04	A_11_P0000020194	Stem cell factor
CXCR4	1.75	5.67E-05	A_11_P0000028093	Chemokine (C-X-C motif) receptor 4
EPHB3	1.70	2.76E-03	A_11_P0000031572	EPH receptor B3
PLA2G4A	1.68	2.49E-02	A_11_P0000024961	Cytosolic phospholipase A2
LECT1	1.66	1.03E-03	A_11_P0000029380	Leukocyte cell derived chemotaxin 1
COL3A1	1.51	1.59E-02	A_11_P0000023936	Collagen, type III, alpha 1
IL15	1.50	1.22E-03	A_11_P0000021657	Interleukin 15
TGFBR3	−1.52	2.75E-04	A_11_P0000033275	Transforming growth factor, beta receptor III
LUM	−1.53	5.23E-03	A_11_P0000027035	Lumican
MICAL-L1	−1.54	2.28E-02	A_11_P0000025935	MICAL-like 1
CTGF	−1.56	4.86E-04	A_11_P0000021765	Connective tissue growth factor
PDE9A	−1.56	2.08E-04	A_11_P0000031313	Phosphodiesterase 9A
ADORA2B	−1.58	4.50E-04	A_11_P0000019672	Adenosine A2b receptor
ITGAV	−1.60	1.90E-04	A_11_P0000031811	Integrin, alpha V
EGFR	−1.61	6.95E-05	A_11_P0000027549	Epidermal growth factor receptor
PDE5	−1.64	3.65E-02	A_11_P0000019906	3',5'-Cyclic GMP Phosphodiesterase
ADM	−1.64	5.68E-05	A_11_P0000019901	Adrenomedullin
LAMC2	−1.64	2.27E-03	A_11_P0000020059	Laminin-5 gamma 2
F3	−1.64	2.42E-02	A_11_P0000020251	Tissue factor (TF)
PPL	−1.66	2.42E-02	A_11_P0000033152	Periplakin
CSPG2	−1.67	7.55E-04	A_11_P0000032208	Chondroitin sulfate proteoglycan 2 (versican)
FLT1	−1.67	9.29E-05	A_11_P0000022693	fms-related tyrosine kinase 1
VWF	−1.68	7.68E-05	A_11_P0000019660	von Willebrand factor
TGFBR2	−1.68	6.99E-05	A_11_P0000022451	Transforming growth factor beta type II receptor
IDH1	−1.69	3.26E-05	A_11_P0000023983	Cytosolic NADP+dependent isocitrate dehydrogenase
CA4	−1.71	1.14E-03	A_11_P0000025419	Carbonic anhydrase IV precursor
TLR4	−1.77	4.57E-04	A_11_P0000019677	Toll-like receptor4 protein
PDGFRA	−1.78	6.94E-05	A_11_P0000020877	Platelet-derived growth factor receptor alpha

Name	Fold	p-value	Systematic Name	Description
FBLN1	−1.78	1.47E-04	A_11_P0000020324	Fibulin 1
FBN1	−1.79	4.04E-04	A_11_P0000023492	Fibrillin 1
EFEMP1	−1.79	5.62E-03	A_11_P0000020441	EGF-containing fibulin-like extracellular matrix protein 1
DCN	−1.80	9.56E-05	A_11_P0000019946	Decorin
STC1	−1.83	1.13E-02	A_11_P0000029912	Stanniocalcin 1
LTBP2	−1.87	1.09E-02	A_11_P0000033795	Latent TGF-beta binding protein 2
PDPN	−1.88	2.90E-04	A_11_P0000019938	Podoplanin
C1QA	−1.89	3.02E-04	A_11_P0000023402	Complement component 1, q subcomponent, A chain
GNAQ	−1.91	3.27E-02	A_11_P0000028288	Guanine nucleotide binding protein, q polypeptide
BPI	−1.92	5.60E-05	A_11_P0000022602	Bactericidal/permeability-increasing protein
CTSS	−2.00	3.96E-06	A_11_P0000019666	Cathepsin S
ITGA11	−2.01	4.97E-03	A_11_P0000023546	Integrin, alpha 11
PPET3	−2.05	2.02E-03	A_11_P0000019670	Preproendothelin-3
MATN2.	−2.11	3.36E-02	A_11_P0000026798	Matrilin 2 precursor
VTN	−2.19	8.82E-04	A_11_P0000025446	Vitronectin
ITGAX	−2.16	7.81E-03	A_11_P0000033071	Integrin, alpha X
GRIA4	−2.31	1.58E-03	A_11_P0000032625	Glutamate receptor ionotropic, AMPA 4
MSR1	−2.38	3.43E-05	A_11_P0000027265	Macrophage scavenger receptor 1
FGFR2	−2.38	1.90E-02	A_11_P0000016005	Fibroblast growth factor receptor 2
THBS1	−2.41	4.39E-04	A_11_P0000031079	Thrombospondin 1
ICAM1	−2.65	2.13E-02	A_11_P0000019508	Intercellular adhesion molecule 1 (CD54)
PAI-1	−2.99	2.10E-03	A_11_P0000024685	Plasminogen activator inhibitor type 1
CSF1R	−3.76	1.54E-04	A_11_P0000032429	Colony stimulating factor 1 receptor
MMRN1	−6.14	6.98E-05	A_11_P0000031372	Multimerin 1